Real-Time Hybrid Simulation Using Shake Tables and Dynamic Actuators

Xiaoyun Shao, A.M.ASCE[1]; Andrei M. Reinhorn, F.ASCE[2]; and Mettupalayam V. Sivaselvan[3]

Abstract: The development and implementation of the real-time hybrid simulation (RTHS), a seismic response simulation method with a combination of numerical computation and physical specimens excited by shake tables and auxiliary actuators, are presented. The structure to be simulated is divided into one or more experimental and computational substructures. The loadings generated by the seismic excitations at the interfaces between the experimental and computational substructures, in terms of accelerations and forces, are imposed by shake tables and actuators in a step-by-step manner at a real-time rate. The measured displacement and velocity responses of the experimental substructure are fed back to determine the loading commands of the next time step. The unique aspect of the aforementioned hybrid simulation method is the versatile implementation of inertia forces and a force-based substructuring. The general formulation of RTHS enables this hybrid simulation method being executed as real-time pseudodynamic (PSD) testing, dynamic testing, and a combination of both, depending on the availability of the laboratory testing equipment and their capacity. The derivation of the general formulation and the corresponding testing system are presented in this paper. Numerical simulation and physical experiment were conducted on the RTHS of a three-story structural model. Simulation and experimental results verify the concept of the proposed general formulation of RTHS and the feasibility of the developed corresponding controller platform. **DOI: 10.1061/(ASCE)ST.1943-541X.0000314.** © *2011 American Society of Civil Engineers.*

CE Database subject headings: Experimentation; Dynamic tests; Pseudodynamic method; Hybrid methods; Simulation; Shake table tests; Seismic effects.

Author keywords: Experimentation; Dynamic tests; Pseudodynamic method; Hybrid methods; General formulation.

Introduction

Although methods of computational dynamic analysis have advanced in recent years, there is still a strong demand for experimental evaluation of the structural performance of complex systems on a large scale. Experimental studies not only enable prediction of a structure's response to future earthquakes but also provide basic information for other types of research, including computational analysis. This is particularly true when the structure or system responds inelastically and/or includes elements whose behavior is strongly rate-dependent, such as damping systems or other nonlinear control devices. To achieve the replication of dynamic behavior of large structural system, researchers have been developing real-time hybrid simulation techniques, during which physical experiments of large-scale structural components/assemblies are subjected to real-time loading while the computational simulations of the remaining structure are executed in parallel with the necessary information transferred in between. These advanced seismic testing methods were recently reviewed by Shing (2008) and can be categorized essentially into two major groups: pseudodynamic (PSD) testing and dynamic testing.

The PSD testing method computationally simulates the inertial effects, employing a numerical model of the prototype structure and applying these inertial effects to the specimen at a slower rate of time. Combined with the substructure techniques, the PSD test was extended to simulate the dynamic response of the whole structural system, in which critical components (such as a restoring force component or an additional damper device) are physically tested while the remaining parts of the structure, together with the inertia effects of the physical specimen, are numerically simulated in a computer (Nakashima et al. 1990; Darby 1999). Both PSD and substructure PSD (or PSD hybrid) tests can be conducted in an extended time frame (Mahin and Shing 1985; Shing et al. 1996) when the computed inertia forces are applied statically or quasi-statically to the specimen; it can also be conducted at a faster or near real-time rate (Shing et al. 2004; Darby et al. 1999; Nakashima 1992) to address the rate-dependent effects within the test structure. Because the dynamic effects of the structure are only numerically simulated, the accuracy of a PSD test result relies greatly on the numerical model of the prototype structure and the integration algorithm. There are also other issues related to the reliability of a PSD testing such as continuous loading using actuators, time delay compensations, and application and stability of numerical algorithms, which have been continuously studied by numerous researchers during the past few years (e.g., Wu 2005; Ahmadizadeh 2008; Wallace 2005; Mercan and Ricles 2007; Stojadinovic 2006; Chen 2009).

On the other hand, inertial effects associated with the mass of the test structure are physically developed during dynamic testing. Both shake table testing (STT) and effective force testing (EFT) are dynamic testing methods. The load applied to the specimen is

[1]Assistant Professor, Dept. of Civil and Construction Engineering, Western Michigan Univ., Kalamazoo, MI 49008-5316 (corresponding author). E-mail: xiaoyun.shao@wmich.edu

[2]Clifford C. Furnas Professor of Structural Engineering, Dept. of Civil and Environmental Engineering, State Univ. of New York, Buffalo, NY 14260-4300.

[3]Assistant Professor, Dept. of Civil, Architectural and Environmental Engineering, Univ. of Colorado, Boulder, CO 80309.

Note. This manuscript was submitted on November 13, 2008; approved on September 12, 2010; published online on September 22, 2010. Discussion period open until December 1, 2011; separate discussions must be submitted for individual papers. This paper is part of the ***Journal of Structural Engineering***, Vol. 137, No. 7, July 1, 2011. ©ASCE, ISSN 0733-9445/2011/7-748–760/$25.00.

predetermined, and no measurements of the specimen's response are required to determine the next step loading command (except for controlling the fidelity of implementation). The test specimen, as a physical model (at small or full scale) representing the prototype structure under investigation, contains all the structural dynamic properties such as mass, damping, and stiffness. Dynamic testing is usually conducted in real-time, although the time rate may be scaled to match the physical scale of the specimen. However, because of the limitation in the shake table's capacity, only a reduced-scale specimen can be tested with STT, the results of which are often difficult to extrapolate to a full-scale prototype structure. Effective force testing (Dimig et al. 1999), on the other hand, is limited to impose dynamic forces to a structural model that can be idealized as lumped-mass systems.

To achieve the realistic inertia effects in the test structure (as opposed to a PSD testing) and to overcome the limitation of shake table capacity, a substructure technique was adopted in shake table testing. Reinhorn et al. (2003, 2005) proposed the real-time dynamic hybrid simulation (RTDHS) to obtain global dynamic response of structural system, during which a portion of the whole structure is physically tested with shake tables applying base motion from the bottom numerical substructure and actuators applying interface forces caused by interaction from the top numerical substructure (Fig. 1). The main advantage of the RTDHS method is that true dynamic response is obtained through this dynamic testing method (as indicated by its name), and there is no restraint in a structural system that can be evaluated with RTDHS, ranging from a lumped-mass system to a distributed-mass system (such as soil-structure system). Neild et al. (2005) conducted an experiment of a mass-spring-damper system by experimentally testing a portion of the mass and numerically modeling the remainder of the mass, the spring, and the damper. A shake table was used as a transfer system introducing the required displacement on the substructure mass to generate partial inertial effects of the whole structural model with the remaining inertial effects numerically simulated. Therefore, this substructure shake table method is a combination of dynamic and PSD testing. Lee et al. (2007) proposed a substructure shake table test of upper substructures, which adopts the upper part of the object structure as the experimental substructure and the lower part as the numerical substructure. The force exerted on the interface of the two separated substructures is calculated online using the feedback from an absolute floor acceleration measurement, and the acceleration at the interface applied to the upper substructure by shake table is calculated with a time history analysis of the numerical substructure. More recently, Ji et al. (2009) proposes a full-scale substructure shake table test to reproduce large-floor responses of high-rise buildings through a rubber-and-mass system to amplify the table motion. Without the auxiliary actuators, the latter two substructure shake table testing methods are limited in testing the upper part of the whole structural model, whereas the shake table imposes interface load from the lower part.

Inspired by the recent advancement in shake table substructure testing methods along with the continuous development of the RTDHS method, a general formulation was proposed for the real-time hybrid simulation (RTHS). Similar to the RTDHS, it integrates dynamic actuators into a shake table substructure test. Whereas RTDHS is restrained in its dynamic loading input configuration in that shake tables impose base motions and actuators introduce top interface forces, RTHS is more flexible in dynamic loading implementation by introducing two sets of splitting coefficients to the general formulation: (1) the load splitting coefficients allow a redistribution of dynamic load between shake tables and dynamic actuators to adapt to the available laboratory equipment; and (2) the mass-splitting coefficients enable versatile implementation of inertial effects during a seismic simulation, resulting in various force-based testing methods, such as real-time PSD substructure testing, dynamic hybrid testing, and a combination of both.

General Formulation for RTHS Method

The RTHS includes the structure to be simulated, divided into an experimental substructure, and one or more computational substructures. Interface forces between the experimental and an upper computational substructure are imposed by actuators. The base excitation motion, or the motion from a computational substructure below, is applied to the experimental substructure by shake tables. Resulting displacements and velocities of the experimental substructure are fed back to the computational engine to determine the interface forces applied to the computational and experimental substructuers for the next time step.

Substructure Formulation

To physically test the experimental substructure with the RTHS method, a numerical model of the whole structural system under investigation is set up, in which the experimental substructure is defined and separated from the complementary computational substructures with the interface parameters identified to calculate the

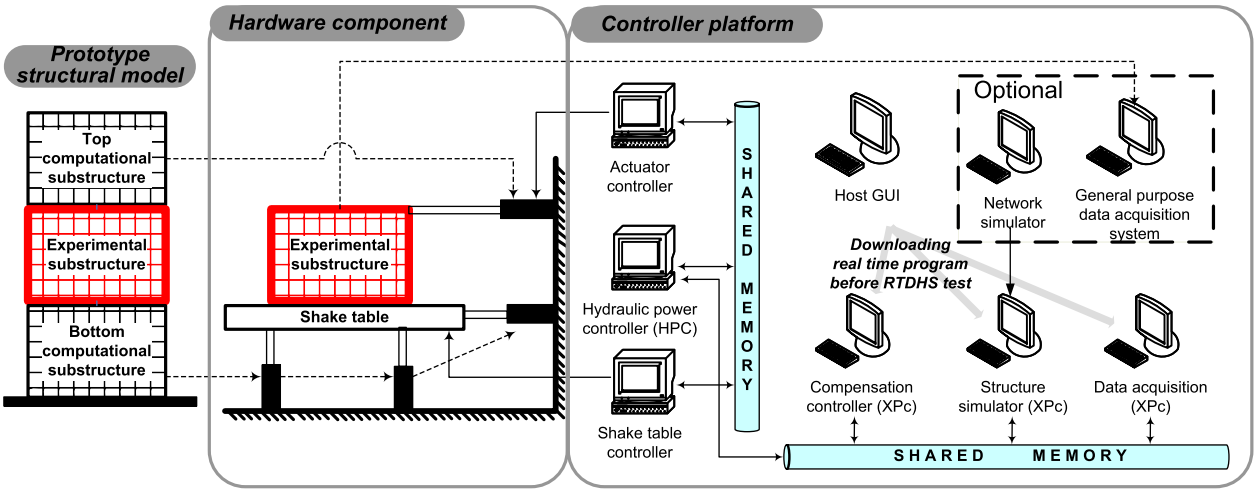

Fig. 1. RTDHS

J. Struct. Eng., 2011, 137(7): 748-760

interface load values, i.e., acceleration commands of shake tables and interface force magnitude of dynamic actuators. Model of each substructure is obtained through partitioning the dynamic properties (i.e., mass, damping and linear stiffness/resorting force matrices) in the equation of motion (EOM) describing the whole structural model (Shao 2007). For the sake of simplicity, derivations are presented for a multistory structural system shown in Fig. 2, and the EOM is given as follows:

$$\mathbf{M}\ddot{\mathbf{x}} + \mathbf{C}\dot{\mathbf{x}} + \mathbf{K}\mathbf{x} = -\mathbf{M}\mathbf{l}\ddot{u}_g \tag{1}$$

where $\mathbf{M}$, $\mathbf{C}$, and $\mathbf{K}$ are the mass, damping, and stiffness matrix of the structural model, $\ddot{u}_g$ is the motion of the ground with respect to the inertial reference frame, and $\mathbf{l}$ is the ground motion scale and direction vector. The damping is assumed to be of the form shown in Fig. 2 to preserve a simple formulation of the computational substructure model. Assuming the whole structure has n degrees-of-freedom (DOFs), in which the top and the bottom computational substructure contains t and b DOFs, respectively, the experimental substructure has n-t-b DOFs. The dynamic property matrices (i.e., $\mathbf{M}$, $\mathbf{C}$ and $\mathbf{K}$) as well as the motion vectors in Eq. (1) are then partitioned based on the substructuring defined in advance as shown in Eq. (2). Elements within the dashed partition lines become the dynamic property matrices (i.e., $\mathbf{M}_3$, $\mathbf{C}_3$, $\mathbf{K}_3$) of each substructure. Elements outside the dashed line in the damping and stiffness matrices (i.e., $-c_{n-t+1}$, $-k_{n-t+1}$), representing the coupling effects between the substructures, are moved to the right side of the EOM. Multiplied with the corresponding motion terms of the interface DOFs, interface forces are formulized (i.e., $\mathbf{P}_1$, $\mathbf{P}_2$, and $\mathbf{P}_3$ in Fig. 2) that need to be applied to each substructure either numerically or physically during RTHS.

$$\begin{bmatrix} m_n & 0 & \cdots & & & \cdots & 0 \\ 0 & \ddots & & & & & \vdots \\ \vdots & \mathbf{M}_3 & m_{n-t+1} & & & & \\ & & m_{n-t} & & & & \\ & & & \ddots & & & \\ & & \mathbf{M}_2 & & m_{b+1} & & \\ & & & & m_b & \ddots & \vdots \\ \vdots & & & & \mathbf{M}_1 & \ddots & 0 \\ 0 & \cdots & & & \cdots & 0 & m_1 \end{bmatrix} \begin{Bmatrix} \ddot{x}_n \\ \ddot{\mathbf{x}}_3 \\ \ddot{x}_{n-t+1} \\ \ddot{x}_{n-t} \\ \ddot{\mathbf{x}}_2 \\ \ddot{x}_{b+1} \\ \ddot{x}_b \\ \ddot{\mathbf{x}}_1 \\ \ddot{x}_1 \end{Bmatrix} + \begin{bmatrix} c_n & -c_n & 0 & \cdots & & \cdots & 0 \\ -c_n & \ddots & & & & & \vdots \\ \vdots & & \mathbf{C}_3 & & & & \\ & & c_{n-t+2}+c_{n-t+1} & & -c_{n-t+1} & & \\ & & -c_{n-t+1} & & c_{n-t+1}+c_{n-t} & -c_{n-t} & \\ & & & & -c_{n-t} & \ddots & \\ & & & & \mathbf{C}_2 & & \\ & & & & c_{b+2}+c_{b+1} & -c_{b+1} & \\ & & & & -c_{b+1} & c_{b+1}+c_b & -c_b \\ & & & & & -c_b & \ddots \\ & & & & & \cdots & -c_2 \\ \vdots & & & & & \mathbf{C}_1 & \\ 0 & \cdots & & & & -c_2 & c_1+c_2 \end{bmatrix} \begin{Bmatrix} \dot{x}_n \\ \dot{\mathbf{x}}_3 \\ \dot{x}_{n-t+1} \\ \dot{x}_{n-t} \\ \dot{\mathbf{x}}_2 \\ \dot{x}_{b+1} \\ \dot{x}_b \\ \dot{\mathbf{x}}_1 \\ \dot{x}_1 \end{Bmatrix}$$

$$+ \begin{bmatrix} k_n & -k_n & 0 & \cdots & & \cdots & 0 \\ -k_n & \ddots & & & & & \vdots \\ \vdots & & \mathbf{K}_3 & & & & \\ & & k_{n-t+2}+k_{n-t+1} & & -k_{n-t+1} & & \\ & & -k_{n-t+1} & & k_{n-t+1}+k_{n-t} & -k_{n-t} & \\ & & & & -k_{n-t} & \ddots & \\ & & & & \mathbf{K}_2 & & \\ & & & & k_{b+2}+k_{b+1} & -k_{b+1} & \\ & & & & -k_{b+1} & k_{b+1}+k_b & -k_b \\ & & & & & -k_b & \ddots \\ & & & & & \cdots & -k_2 \\ \vdots & & & & & \mathbf{K}_1 & \\ 0 & \cdots & & & & -k_2 & k_2+k_1 \end{bmatrix} \begin{Bmatrix} x_n \\ \mathbf{x}_3 \\ x_{n-t+1} \\ x_{n-t} \\ \mathbf{x}_2 \\ x_{b+1} \\ x_b \\ \mathbf{x}_1 \\ x_1 \end{Bmatrix} = - \begin{bmatrix} m_n & 0 & \cdots & & & \cdots & 0 \\ 0 & \ddots & & & & & \vdots \\ \vdots & \mathbf{M}_3 & m_{n-t+1} & & & & \\ & & m_{n-t} & & & & \\ & & & \ddots & & & \\ & & \mathbf{M}_2 & & m_{b+1} & & \\ & & & & m_b & \ddots & \vdots \\ \vdots & & & & \mathbf{M}_1 & \ddots & 0 \\ 0 & \cdots & & & \cdots & 0 & m_1 \end{bmatrix} \mathbf{l}\ddot{u}_g \tag{2}$$

Three EOMs corresponding to three substructures are then derived from the partitioned equation as summarized in Fig. 2. $\mathbf{M}_3$, $\mathbf{C}_3$, $\mathbf{K}_3$, and $\mathbf{M}_1$, $\mathbf{C}_1$, $\mathbf{K}_1$ are the mass, damping, and stiffness matrices of the top and bottom computational substructures that will be numerically simulated. $\mathbf{P}_3$ and $\mathbf{P}_1$ are the interface forces on the computational substructures. In a closed-loop implementation, $\mathbf{P}_3$ and $\mathbf{P}_1$ are calculated in real-time based on the displacement and velocity feedback at the interface of the experimental substructure $(x_{n-t}, \dot{x}_{n-t}, x_{b+1}, \dot{x}_{b+1})$ and the interface force parameters $(c_{n-t+1}, k_{n-t+1}, c_{b+1}, k_{b+1})$ defined beforehand. Simulated responses are then determined at each step. The structural damping and stiffness of the computational model are assumed to be linear, consistent with the intention of conducting substructure testing in that the computational substructures are the parts within the whole structural system that usually have simple and predictable structural performance (i.e., linear response subjected to large load input) and therefore can be numerically modeled economically with relatively high accuracy. Nevertheless, computational substructures can be nonlinear if such response is expected and a validated computational model is available to be integrated in the RTHS testing system.

In the EOM of the experimental substructure in Fig. 2, the interface force $\mathbf{P}_2$ and the base motion $\ddot{u}_b$ are shown in the solid line boxes. u_i and x_i are the motions of the i-th story with respect to the inertial reference frame and the ground, respectively. The motion variable $\mathbf{x}_{2b} = [\mathbf{x}_2 - x_b\mathbf{l}]$, which is the relative displacement vector between the experimental substructure and the top DOF of the bottom computational substructure (bth DOF), is introduced. $\mathbf{l}$ is a vector of the same order as $\mathbf{x}_2$ with each element equal to unit. During a closed-loop RTHS test, the dynamic property matrices associated with the experimental substructure ($\mathbf{M}_2$, $\mathbf{C}_2$, $\mathbf{K}_2$) will be physically represented by using the test specimen, whereas the interface load in the form of base acceleration $\ddot{u}_b$ and top interface force $\mathbf{P}_2$ will be determined from the simulated responses of the computational substructures (i.e., $\dot{x}_{n-1+t}$, x_{n-1+t}, and $\ddot{x}_b$) and the measured responses $(\dot{x}_{n-1}, x_{n-1})$ of the experimental substructure from the previous step. Therefore, the linear format of the damping and stiffness matrices $\mathbf{C}_2$, $\mathbf{K}_2$ used herein is only for the simple representation that will not be accurately formulated and utilized in a closed-loop implementation of RTHS. However, during the test preparation, experimental substructure models are usually estimated to set the loading devices' limits and to design the appropriate test rig.

J. Struct. Eng., 2011, 137(7): 748-760

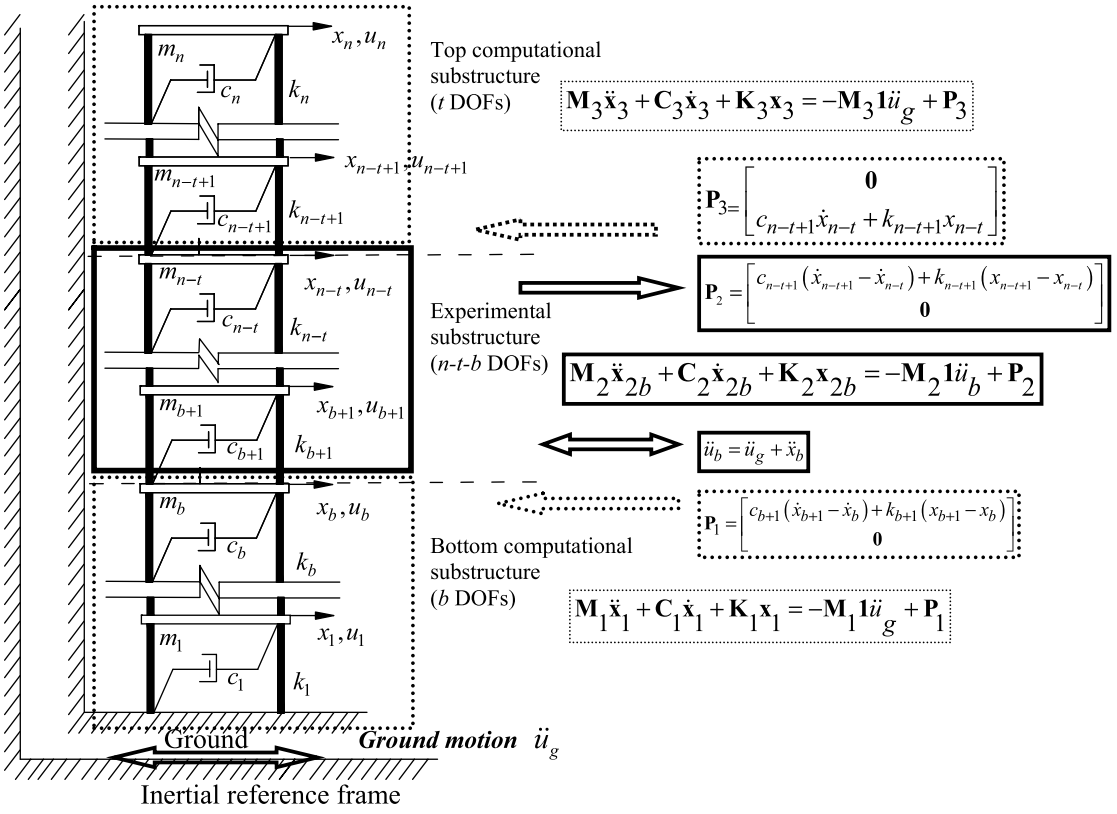

Fig. 2. Multistory structural model and substructure formulation of RTHS

With advancing of time steps, the responses (i.e., displacement, velocity, and acceleration) of the global structural system subjected to the ground acceleration excitation $\ddot{u}_g$ will be obtained at the end of the hybrid simulation. Thus, equations in Fig. 2 represent the substructure formulation of RTHS for a multistory structural model.

General Formulation of RTHS

While the development of the original RTDHS progressed, the seismic simulation method involving both shake tables and dynamic actuators was extended to a general real-time force-based substructure testing method. Various modern seismic testing methods and techniques as described in the Introduction, i.e., dynamic testing, pseudodynamic testing, or even a hybrid approach of dynamic and pseudodynamic testing, can be mathematically defined using the general formulation of RTHS and implemented by using the RTDHS testing system with minor modification in the controller.

By introducing two sets of splitting coefficients to the EOM of the experimental substructure (the equation in the solid line box in Fig. 2), the general formulation of RTHS of a multistory structural model is given as follows:

$$(\mathbf{I}-\boldsymbol{\alpha}_m)(\mathbf{M}_2\ddot{\mathbf{x}}_{2b})+\mathbf{C}_2\dot{\mathbf{x}}_{2b}+\mathbf{K}_2\mathbf{x}_{2b}-(\mathbf{I}-\boldsymbol{\alpha}_m)\mathbf{M}_2\mathbf{l}\underbrace{[\alpha_l\ddot{u}_b]}_{\text{Base Acceleration}}+\underbrace{\{-(\mathbf{I}-\boldsymbol{\alpha}_m)\mathbf{M}_2\mathbf{l}[(1-\alpha_l)\ddot{u}_b]-\boldsymbol{\alpha}_m\mathbf{M}_2\ddot{\mathbf{x}}_{2b}-\boldsymbol{\alpha}_m\mathbf{M}_2\mathbf{l}\ddot{u}_b+\mathbf{P}_2\}}_{\text{Applied Force}} \tag{3}$$

where $\mathbf{I}$ is the identity matrix. $\mathbf{M}_2$, $\mathbf{C}_2$, $\mathbf{K}_2$ are the mass, damping, and stiffness matrices of the experimental substructure and $\ddot{\mathbf{x}}_{2b}, \dot{\mathbf{x}}_{2b}$, and $\mathbf{x}_{2b}$ define the relative motion between the DOFs of the experimental substructure with respect to the top DOF of the bottom substructure. $\mathbf{P}_2$ is the interface force from the top substructure, and $\ddot{u}_b$ is the acceleration response of the bth DOF in the bottom substructure representing the base motion input to the experimental substructure. The base motion splitting coefficient α_l is a scalar, and the mass-splitting coefficient matrix $\boldsymbol{\alpha}_m$ is a diagonal matrix of the order $(n-t-b)$. Values of α_l and the diagonal elements in $\boldsymbol{\alpha}_m$ vary between 0 and 1, resulting in different implementation cases listed in Table 1. Three categories of testing methods (PSD, dynamic, and quasi-dynamic) are identified based on the mass-splitting coefficient matrix $\boldsymbol{\alpha}_m$.

When $\boldsymbol{\alpha}_m=\mathbf{I}$, no physical mass is represented in the experimental substructure; the inertia effects of the mass are numerically simulated and applied to the specimen as external forces by the actuators with no input from shake tables. This type of test is known as PSD testing. Similar to a conventional displacement-based PSD test, this force-based PSD test requires an estimated mass of the structural model to numerically determine the inertial effects, whereas the damping and restoring force components of the model are physically tested. However, no integration algorithm is required in this force-based PSD test. Instead, the acceleration response of the experimental substructure ($\ddot{\mathbf{x}}_2$) is fed back in real time to determine the inertial forces ($-\mathbf{M}_2\ddot{\mathbf{x}}_{2b}$) caused by the interface motion from the bottom computational substructure. In addition, the applied forces include both the effective forces caused by the base motion ($-\mathbf{M}_2\mathbf{l}\ddot{u}_g$) and the interface forces ($\mathbf{P}_2$) from the top experimental substructure.

When $\boldsymbol{\alpha}_m=\mathbf{0}$, full mass required for seismic simulation is presented in the physical experimental substructure without virtual mass. Therefore, no supplementary inertia forces are applied to the specimen. This test category, with full physical mass, is defined as dynamic testing during which the inertia effects are physically (naturally) developed. Moreover, when the base motion splitting

J. Struct. Eng., 2011, 137(7): 748-760

Table 1. Real-Time Hybrid Simulation—Loading Implementation Cases

Test structural model		Total dynamic load		
$(\mathbf{I}-\boldsymbol{\alpha}_m)(\mathbf{M}_2\ddot{\mathbf{x}}_{2b})+\mathbf{C}_2\dot{\mathbf{x}}_{2b}+\mathbf{K}_2\mathbf{x}_{2b}$		$-(\mathbf{I}-\boldsymbol{\alpha}_m)\mathbf{M}_2\mathbf{l}\underbrace{[\alpha_l\ddot{u}_b]}_{\text{Base Acceleration}}+\underbrace{\{-(\mathbf{I}-\boldsymbol{\alpha}_m)\mathbf{M}_2\mathbf{l}[(1-\alpha_l)\ddot{u}_b]-\boldsymbol{\alpha}_m\mathbf{M}_2\ddot{\mathbf{x}}_{2b}-\boldsymbol{\alpha}_m\mathbf{M}_2\mathbf{l}\ddot{u}_b+\mathbf{P}_2\}}_{\text{Applied Force}}$		
Mass splitting	Physical model	Load splitting	Shake table	Actuator
Pseudodynamic	$\mathbf{C}_2\dot{\mathbf{x}}_{2b}+\mathbf{K}_2\mathbf{x}_{2b}$	N/A	0	$-\mathbf{M}_2\ddot{\mathbf{u}}_2$[a]$+\mathbf{P}_2$
$\boldsymbol{\alpha}_m=\mathbf{I}$				
Dynamic	$\mathbf{M}_2\ddot{\mathbf{x}}_{2b}+\mathbf{C}_2\dot{\mathbf{x}}_{2b}$	$\alpha_l=0$	0	$-\mathbf{M}_2\mathbf{l}\ddot{u}_b+\mathbf{P}_2$
$\boldsymbol{\alpha}_m=\mathbf{0}$	$+\mathbf{K}_2\mathbf{x}_{2b}$	$\alpha_1=1$	$\ddot{u}_b$	$\mathbf{P}_2$
		$0<\alpha_l<1$	$\alpha_l\ddot{u}_b$	$-\mathbf{M}_2\mathbf{l}(1-\alpha_l)\ddot{u}_b+\mathbf{P}_2$
Quasi-dynamic	$(\mathbf{I}-\boldsymbol{\alpha}_m)(\mathbf{M}_2\ddot{\mathbf{x}}_{2b})$	$\alpha_l=0$	0	$-\mathbf{M}_2\mathbf{l}\ddot{u}_b-\boldsymbol{\alpha}_m(\mathbf{M}_2\ddot{\mathbf{x}}_{2b})+\mathbf{P}_2$
$\mathbf{0}<\boldsymbol{\alpha}_m<\mathbf{I}$	$+\mathbf{C}_2\dot{\mathbf{x}}_{2b}+\mathbf{K}_2\mathbf{x}_{2b}$	$\alpha_l=1$	$\ddot{u}_b$	$-\boldsymbol{\alpha}_m\mathbf{M}_2\ddot{\mathbf{u}}_2+\mathbf{P}_2$
		$0<\alpha_l<1$	$\alpha_l\ddot{u}_b$	$-(\mathbf{I}-\boldsymbol{\alpha}_m)\mathbf{M}_2\mathbf{l}\{(1-\alpha_l)\ddot{u}_b\}$
				$-\boldsymbol{\alpha}_m\mathbf{M}_2\ddot{\mathbf{u}}_2+\mathbf{P}_2$

[a]Absolute acceleration vector with respect to the inertial reference frame $\ddot{\mathbf{u}}_2=\ddot{\mathbf{x}}_2+\mathbf{l}\ddot{u}_g$.

coefficient α_l takes different values, three different load implementation cases are derived in this RTHS testing category:

- $a_l=0$, shake table (or base) is not excited and the entire dynamic load including both effective forces ($-\mathbf{M}_2\mathbf{l}\ddot{u}_b$), and the interface forces ($\mathbf{P}_2$) are applied to the experimental substructure by using the actuators attached to the mass of each DOF. This is recognized as effective force testing method with substructuring.
- $\alpha_l=1$, the base acceleration ($\ddot{u}_b$), as a combination of ground and bottom substructure motion input, is reproduced by shake table without contribution to the effective forces. This is the shake table substructuring testing. When an upper substructure is included, the interface forces $\mathbf{P}_2$ resulting from the complementary top computational substructure is applied by actuators at the interface DOFs. Then it becomes the conventional real-time dynamic hybrid simulation (Reinhorn et al. 2005).
- Beside the aforementioned two special cases, the base motion can be applied in part by shake table and in part by actuators. Several strategies may be used to split the dynamic loading between shake table and actuators as proposed by Kausel (1998a, b). In fact, the characteristics of the splitting coefficients can be chosen to optimize the total power needed by the testing system or to achieve other mechanical advantages.

The third category, defined as quasi-dynamic testing, takes place when $\mathbf{0}<\boldsymbol{\alpha}_m<\mathbf{I}$ (not all the diagonal entries in $\boldsymbol{\alpha}_m$ equal to zero or unity) when the required mass is divided into physical mass and virtual mass. Quasi-dynamic testing is a combination of dynamic and PSD testing during which the inertia forces related to the virtual mass are simulated numerically and applied as external forces. Similar to the force-based PSD testing, the acceleration response of the experimental substructure is fed back to determine the virtual inertial forces ($-\boldsymbol{\alpha}_m\mathbf{M}_2\ddot{\mathbf{u}}_2$). This hybrid approach allows for the imposition of dynamic effects when the physical testing facilities are limited in capacity (i.e., specimen mass limitation of shake tables). When α_l takes different values, the same three load implementation cases as for the dynamic testing are derived and listed in Table 1.

Thus, Eq. (3) represents the general formulation of RTHS, in which ideally all seven cases shall produce the same dynamic responses of the structural system subjected to dynamic excitations. Note that taking different values of the splitting coefficient matrices $\boldsymbol{\alpha}_m$ and α_l yields three testing categories and seven loading implementation cases implying the simultaneous numerical simulation and physical experiment. A closed-loop implementation of the RTHS with substructure will require all three measured responses (displacement, velocity, and acceleration) of the experimental substructure fed back to the controller to determine either the interface forces or the inertial forces related to the virtual mass.

Numerical Simulation

To validate the general formulation of the RTHS method, a three-story shear model structure (Fig. 3) was designed and physically tested later . The mass, damping, and stiffness of each story are listed in Table 2, in which the damping is assumed to be viscous. The equation of motion (EOM) of the whole structural model was set up first. The same notation is used as defined in the substructure formulation:

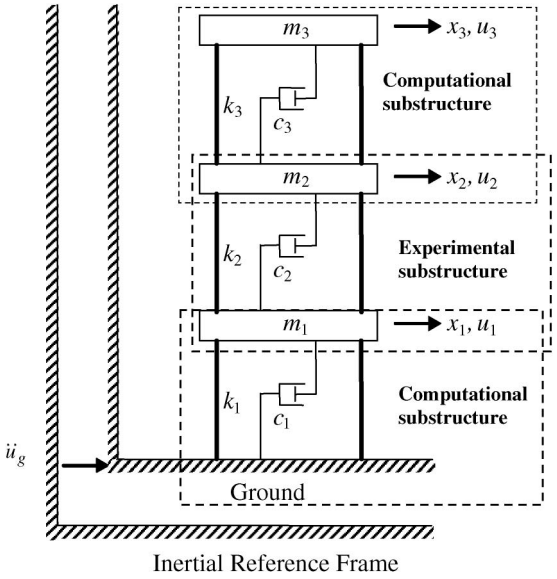

Fig. 3. Three-story hybrid simulation model

Table 2. Dynamic Properties of the Three-Story Model

Story/ Mode	Mass (kips·s^2/in.)	Damping (kips s/in.)	Stiffness (kips/in.)	Natural frequency (Hz)
1st	8.8×10^{-4}	1.19×10^{-3}	0.633	1.55
2nd	4.4×10^{-4}	1.19×10^{-3}	0.126	2.91
3rd	2.2×10^{-4}	1.19×10^{-3}	0.032	4.87

$$\begin{bmatrix} m_3 & 0 & 0 \\ 0 & m_2 & 0 \\ 0 & 0 & m_1 \end{bmatrix} \begin{Bmatrix} \ddot{x}_3 \\ \ddot{x}_2 \\ \ddot{x}_1 \end{Bmatrix} + \begin{bmatrix} c_3 & -c_3 & 0 \\ -c_3 & c_2 + c_3 & -c_2 \\ 0 & -c_2 & c_1 + c_2 \end{bmatrix} \begin{Bmatrix} \dot{x}_3 \\ \dot{x}_2 \\ \dot{x}_1 \end{Bmatrix} + \begin{bmatrix} k_3 & -k_3 & 0 \\ -k_3 & k_2 + k_3 & -k_2 \\ 0 & -k_2 & k_1 + k_2 \end{bmatrix} \begin{Bmatrix} x_3 \\ x_2 \\ x_1 \end{Bmatrix} = -\begin{bmatrix} m_3 & 0 & 0 \\ 0 & m_2 & 0 \\ 0 & 0 & m_1 \end{bmatrix} \ddot{u}_g \tag{4}$$

Defining the first and third floor as the computational substructures and the second floor as the physical experimental substructure, Eq. (4) is simply partitioned with dividing lines separating each column and row in the property matrices and the motion vectors. Note that in this case, DOFs of the third and first story are not only associated with the computational substructures but serving as the interface DOFs as well. By considering the influence between the substructures, the EOM of each substructure was derived from the partitioned EOM as

$$\begin{aligned} &\text{Computational} \begin{cases} m_3\ddot{x}_3 + c_3\dot{x}_3 + k_3x_3 = -m_3\ddot{u}_g + P_3 = -m_3\ddot{u}_g + k_3x_2 + c_3\dot{x}_2 \\ m_1\ddot{x}_1 + c_1\dot{x}_1 + k_1x_1 = -m_1\ddot{u}_g + P_1 = -m_1\ddot{u}_g + k_2x_{21} + c_2\dot{x}_{21} \end{cases} \\ &\text{Experimental } m_2\ddot{x}_{21} + c_2\dot{x}_{21} + k_2x_{21} = -(m_2\ddot{u}_g + m_2\ddot{x}_1) + (k_3x_{32} + c_3\dot{x}_{32}) = -m_2\ddot{u}_1 + P_2 \end{aligned} \tag{5}$$

For a hybrid simulation with a single DOF experimental substructure, the mass-splitting coefficient matrix $\boldsymbol{\alpha}_m$ was reduced to a scalar α_m. Also, beside α_m and α_l as defined previously, one more coefficient α_p was introduced to split the interface force between shake table and actuator. Thus, the general formulation became

$$[1-\alpha_m]m_2\ddot{x}_{21} + c_2\dot{x}_{21} + k_2x_{21} = -[1-\alpha_m]m_2\underbrace{\left[\frac{\alpha_l\ddot{u}_1}{(1-\alpha_m)} - \frac{\alpha_pP_2}{(1-\alpha_m)m_2}\right]}_{\text{Base acceleration}}\underbrace{-[1-\alpha_l]m_2\ddot{u}_1 - \alpha_m(m_2\ddot{x}_{21}) + [1-\alpha_p]P_2}_{\text{Applied force}} \tag{6}$$

Taking values of the three coefficients between 0 and 1 in Eq. (6) resulted in various loading implementations cases corresponding to different types of seismic simulation methods. Five cases listed in Table 3 (except for Case 2E) were solved numerically ranging from PSD, quasi-dynamic, and dynamic testing methods to validate the general formulation proposed herein. Numerical simulations of the three-story RTHS test were conducted in the time domain with models created in MATLAB/*Simulink*. The three-story structure is modeled linearly using the dynamic properties listed in Table 2. Ground acceleration from the Northridge earthquake of January 17, 1994, recorded at Santa Monica City Hall at 90 °N-S, with a peak ground acceleration of 0.84 g, was input as the base excitation motion. The flowchart of the simulation program is shown in Fig. 4. Solid lines represent the data being transferred are either predefined or simulated by the computational model, and dashed lines represent measured data of the experimental substructure being fed back to determine the interface forces, base motions or inertia forces related to virtual mass. A closed-loop implementation was adopted in this numerical simulation to demonstrate the general formulation and the simulation was executed at 1,024 Hz.

The relative displacement responses of each story from the five different loading implementation cases are plotted in Fig. 5. The results perfectly match each other showing that the proposed general formulation enables the RTHS test to be implemented with versatile loading configurations while still achieves the goal of seismic simulation that is to estimate/predict the dynamic responses of the structural system/components subjected to dynamic excitations. The physical RTHS implementation of the same three-story structure model is presented in the "Experimental Demonstration" section.

RTHS Testing System

The architecture of the testing system developed for the real-time dynamic hybrid simulation method (Reinhorn et al. 2005) was modularly designed capable of conducting most real-time hybrid seismic simulation, including displacement-based PSD testing (Ahmadizadeh et al. 2008) and the force-based RTHS proposed herein. A schematic of this testing system is shown in Fig. 1. The hardware components required by RTHS, as indicated in the middle box, consist of the physical experimental substructure (the specimen), shake table, and dynamic actuator. The components in the right box illustrate the controller platform required to simulate and implement the forces and/or motions at the interface to the specimen defined by the general formulation.

The controller platform uses multiple computational systems (PCs), including the following modules (see Fig. 6): (1) a data

Table 3. Implementation Cases of Numerical Simulation (N) and Validation Experiments (E)

Loading cases						Applied loading	
	Type		α_m	α_l	α_p	Shake table (base acceleration)	Actuator (applied force)
1		Quasi-dynamic	0.77	0	0	0	$-m_2\ddot{u}_1 - 0.77m_2\ddot{x}_{21} + P_2$
2N		Pseudodynamic	1	0	0	0	$-m_2\ddot{u}_1 - m_2\ddot{x}_{21} + P_2$
2E	Dynamic	RTHS general	0	0.5	0.5	$0.5\ddot{u}_1 - 0.5\ P_2/m_2$	$-0.5m_2\ddot{u}_1 + 0.5P_2$
3		EFT substructure	0	0	0	0	$-m_2\ddot{u}_1 + P_2$
4		STT substructure	0	1	1	$\ddot{u}_1 - P_2/m_2$	0
5		RTDHS conventional	0	1	0	$\ddot{u}_1$	P_2

J. Struct. Eng., 2011, 137(7): 748-760

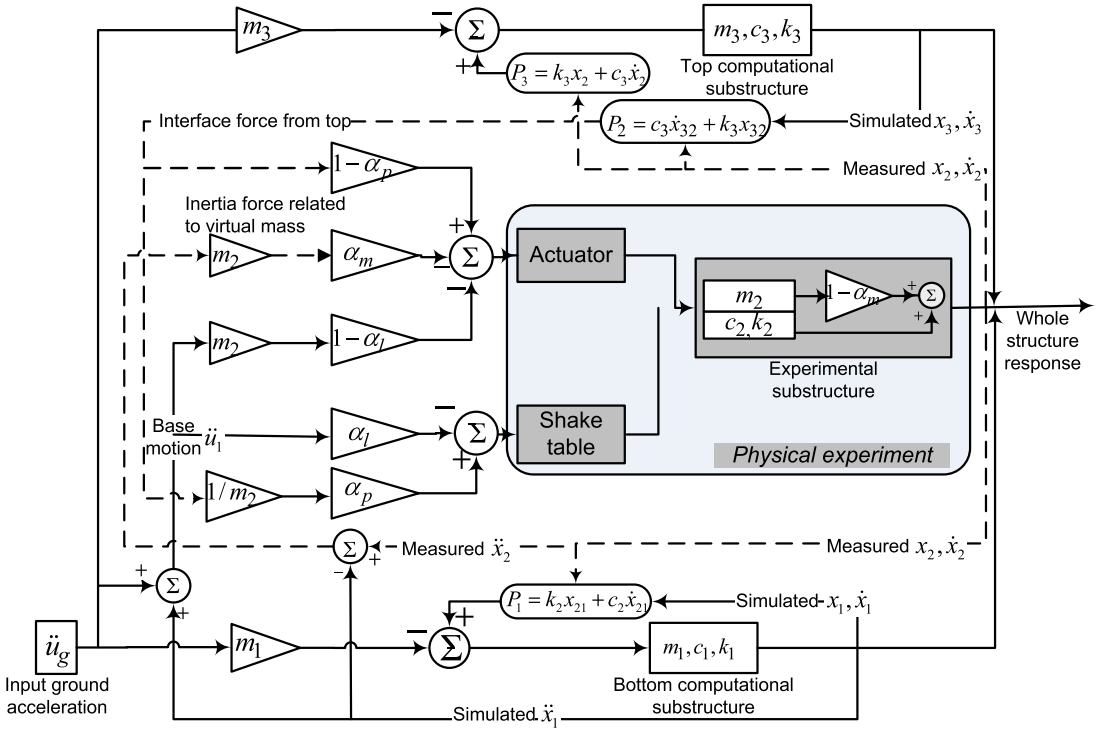

Fig. 4. Numerical simulation flowchart

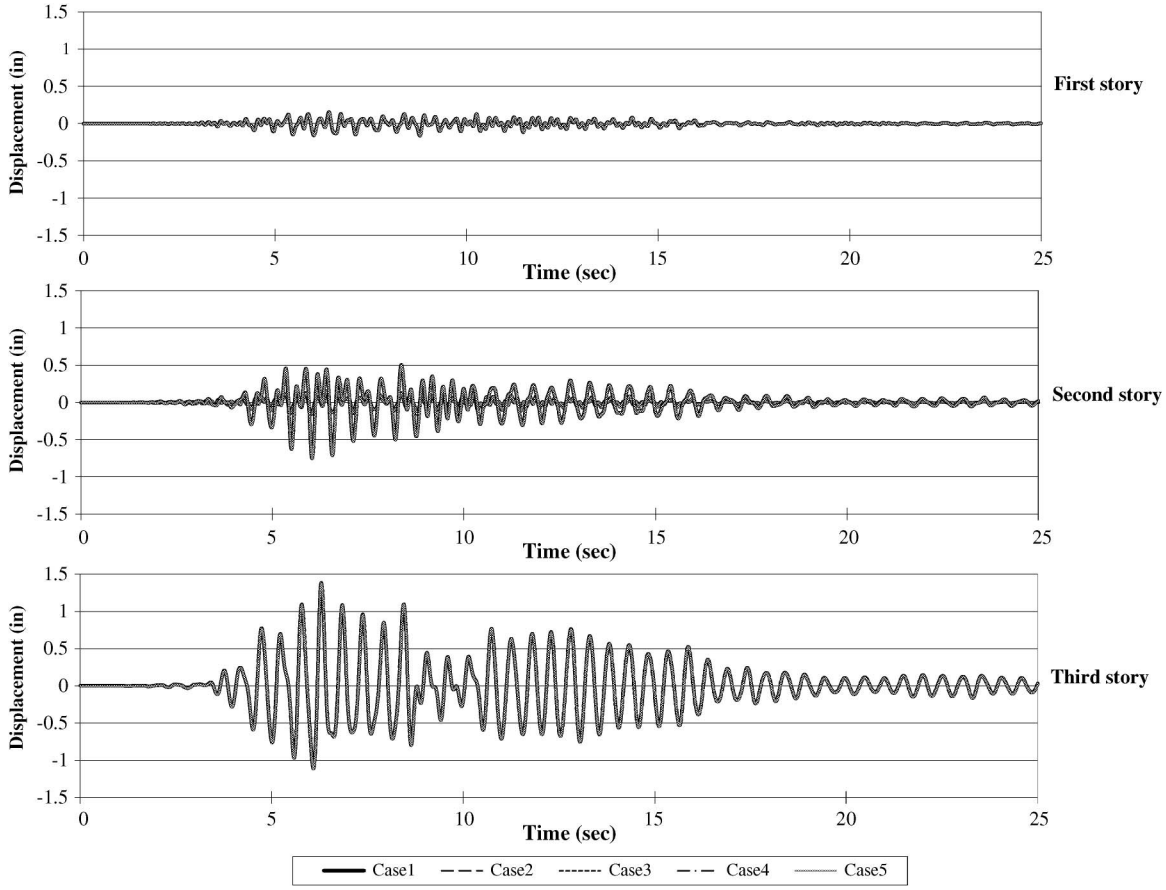

Fig. 5. Numerical simulation results of the three-story RTHS

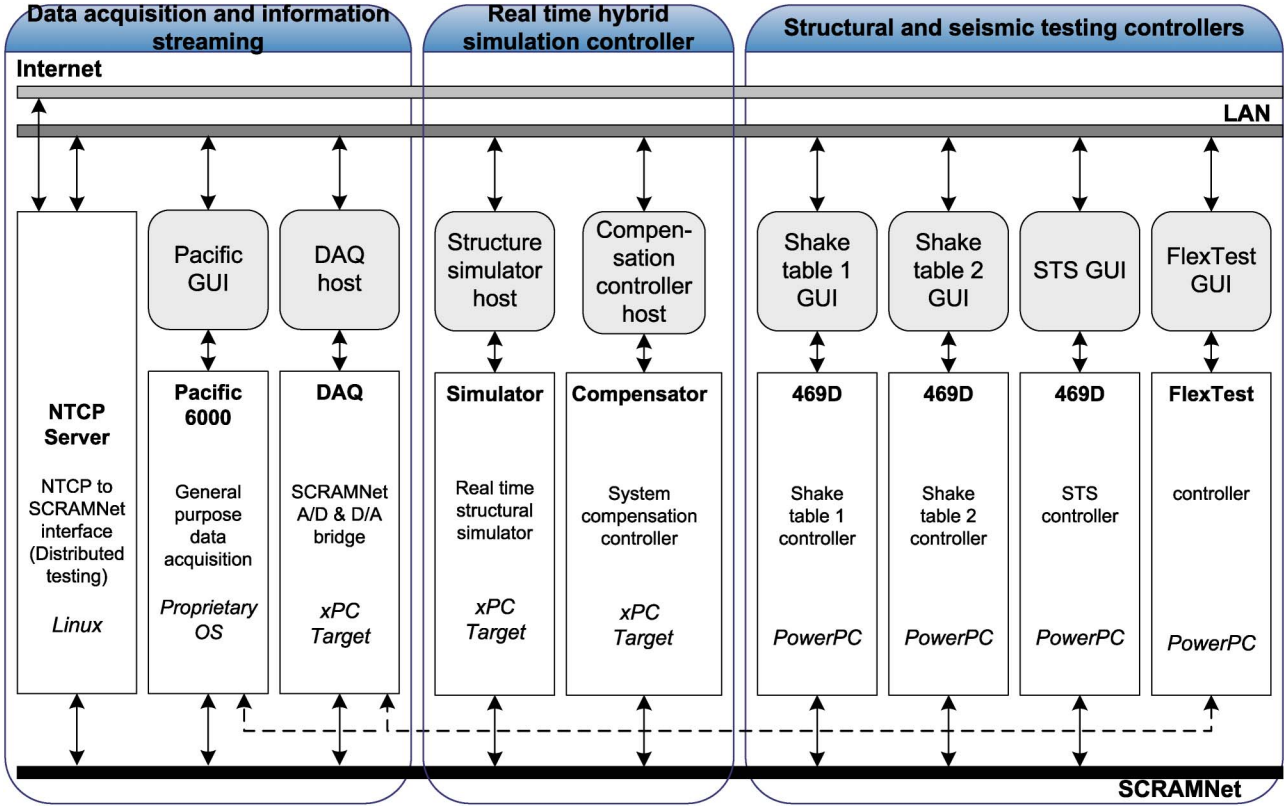

Fig. 6. Controller platform modules

acquisition and information streaming module, which collects simulation data from both experimental and computational substructures and send them to the shared memory; (2) a structural and seismic testing controllers module, which controls individual loading equipment—shake tables and dynamic actuators; (3) a real-time hybrid simulation controller module, which simulates analytically the computational model and determines the compensated commands of loading equipment; and (4) a data communication module, which provides data transferring paths at different levels. An example of the RTHS controller platform developed at the Structural Engineering and Earthquake Simulation Laboratory (SEESL), University at Buffalo, is shown in Fig. 6. Each component [with the exception of the NEESgrid-Teleoperations Control Protocol (NTCP) Server on the left] consists of a host PC that serves as the interface to a real-time microprocessor using the Internet protocols. The arrows in the plot represent the data transfer paths among the computers through the Data communication module at three levels of transferring speed: Internet, local area network (LAN), and the shared common random access memory network (SCRAMNet).

Real-Time Hybrid Simulation Controller

The real-time hybrid simulation controller in Fig. 6 performs various analytical simulation and compensation control functions during RTHS. The primary flow diagram is presented in Fig. 7

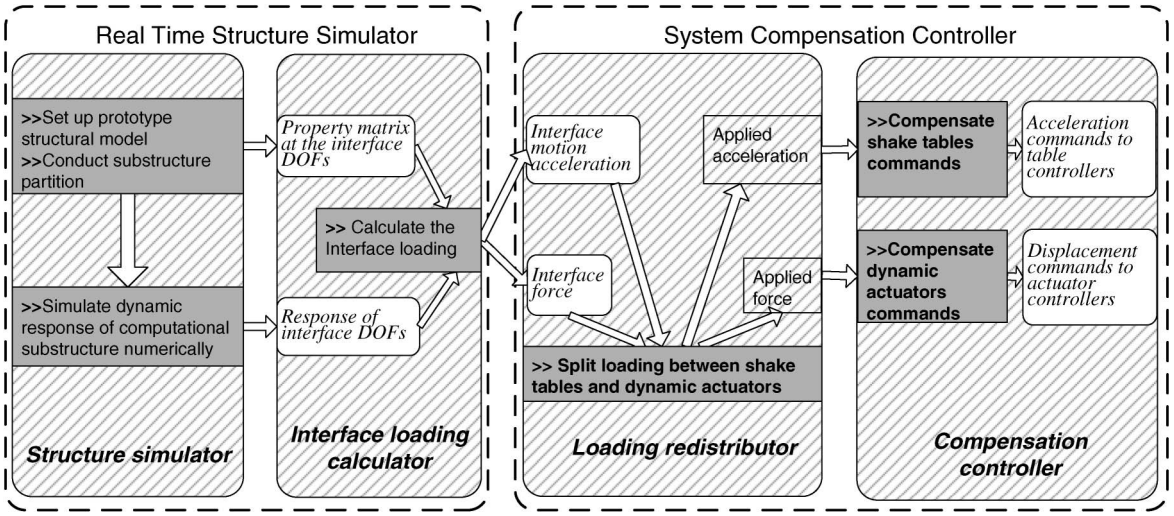

Fig. 7. Flow diagram of real-time hybrid simulation controller

J. Struct. Eng., 2011, 137(7): 748-760

showing two submodules, the real-time structure simulator (RTSS) and the system compensation controller (SCC), with their respective tasks. The module based RTSS evaluates the numerical models of the computational substructures and calculates the interface load (forces/base motions) on the basis of the predefined excitation history, the measured responses of the experimental substructure, and the simulated responses of the computational substructures. RTSS performs off-line tasks such as (1) structural model assembly; (2) substructure partition and interface parameter definition; and online tasks as (3) time-stepping numerical simulation; and (4) interface load calculation. Shao (2007) presented detailed numerical considerations and flowchart of the RTSS programming for both linear and nonlinear experimental substructure. The SCC first redistributes the load between shake tables and actuators on the basis of the predefined splitting coefficients $\boldsymbol{\alpha}_m$ and α_l. Then it generates compensated commands that will be sent to the structural and seismic testing controllers through SCRAMNet.

Control Strategy in System Compensation Controller

Most recent constructed shake tables have an acceleration control mode to reproduce the predefined acceleration records to generate accurate inertia effects within the physical specimen; and during effective force testing, actuators apply effective forces (the product of the input ground acceleration and the mass of the specimen). The RTHS as a dynamic testing method utilizing both loading equipment requires the interface loads applied by the shake table in the form of acceleration and applied by the actuators in the form of force. Therefore, actuators in RTHS have to be operated in dynamic force control instead of displacement control, as in most PSD tests. Moreover, shake tables usually move large displacements to achieve the desired acceleration command, thus actuators when installed against the reaction wall off the shake table, have to move along with the shake table during RTHS. The displacement command of the actuator consists of the shake table displacement and an additional displacement used to apply the interface force to the specimen whose base is moving with the shake table. This additional displacement determined by the interface force is usually small compared to the total motion of the actuator, so the control of such interface force is difficult, unless the actuators are using force control.

However, dynamic force control of hydraulic actuators, especially across the resonant frequency ranges near the natural frequencies of the specimen, is difficult to achieve. This control is sensitive to acceleration and force measurements, modeling of the compressibility of fluid, nonlinearities of the servo control system, and other issues as indicated by Dimig (1999) and Shield and French (2001). To overcome the aforementioned difficulties, a force control method implemented using added compliance and displacement compensation was proposed (Sivaselvan et al. 2008). The actuator itself operates in closed-loop displacement control, and to obtain force control, a displacement compensation feedback loop with the structural displacement response (x_{st}) is needed (see Fig. 8). The force applied to the testing specimen is then accurately calculated using Hooke's Law by multiplying the measured deformation of the added compliance and its stiffness (K_{LC}). Smith's predictor was adopted to minimize adverse effect of time delay in displacement feedback. Detailed theoretical development and the laboratory implementation of the approach are presented by Sivaselvan (2008). Such a method was accepted in the SCC of the RTHS testing system and used in the validation experiment subsequently discussed.

Experimental Demonstration

Two series of the RTDHS tests with two different testing setups (different shake tables and actuators) were performed on the same midscale two-story structure by Reinhorn et al. (2005), in which the first story was built on the shake table (experimental substructure) and the second story was simulated (computational substructure). The shake tables were used only to input the base motion (i.e., ground acceleration in this case), and the actuators imposed the interface forces from the above second story. Test results demonstrated the concept of the RTDHS and the corresponding testing system. To further validate the general formulation of RTHS, which allows more versatile load implementation cases as compared to RTDHS, a pilot-scale three-story structural model was designed, numerically simulated (see "Numerical Simulation" section), and physically tested. Because of the limitation of the shake table controller, open-loop implementation of RTHS substructure formulation was conducted. A numerical model of the whole three-story structural model was formulated in the RTSS, and the simulated responses subjected to the seismic input were solved step-by-step in real time. The interface forces applied to the experimental substructure were then calculated using substructure formulation Eq. (5) on the basis of the numerically simulated responses of both computational and experimental substructures (the second story). No physical specimen's responses were used in the interface load calculation. The base acceleration and the interface force were then transferred to the SCC through the SCRAMNet where the loading splitting coefficients α_m, α_l, and α_p were predefined. Displacement feedback of the test specimen was required by force control of the acutator, and the Smith's predictor was used to compensate

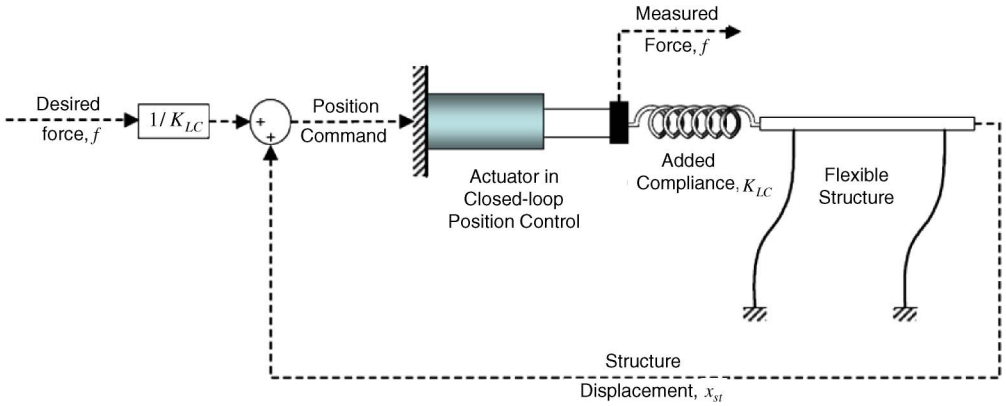

Fig. 8. Dynamic force control of actuator

J. Struct. Eng., 2011, 137(7): 748-760

the time delay as discussed in the control strategy. Five selected implementation cases were tested. Experimental results in both frequency and time domain of the physical substructure are presented and compared with the numerical results.

Test Setup

The physical test setup used in this three-story hybrid simulation consists of a dynamic actuator, a unidirection shake table, and a SDOF frame structure (see Fig. 9). An MTS Systems Corporation 252.22c two-stage servovalve, 2.5 gpm (9.5 l/ min), and an MTS Systems Corporation 204.09 actuator, 2.2 kips (9.8 kN) capacity, 4 in. (101.6 mm) stroke, are used as the dynamic actuator to impose the applied interface forces after load redistribution. The actuator driving the shake table has a dynamic force rating of 21 t (9.8 kN) and a stroke of 300 mm (±150 mm). Both actuators were controlled by the generic MTS Systems Corporation 469 STS real-time hybrid structural test system (MTS Systems Corporation 2003) designed for the Network for Earthquake Engineering Simulation (NEES) services at University at Buffalo. The SCC was implemented in this generic closed-loop system using MATLAB/Simulink, *xPC Target* and SCRAMNet. The right plot of Fig. 9 shows the added compliance connection between the actuator and the specimen to enable force control as illustrated in Fig. 8. As listed in Table 2, the full mass required by dynamic simulation of the experimental substructure (second story) is 4.4×10^{-4} kips $\times$ s^2/in. (79.1 kg) and was provided by five lead blocks in addition to the steel plate. A reduced-mass specimen was obtained by removing the lead bricks for the demonstration of the quasi-dynamic hybrid testing. The physical mass remaining in the reduced-mass specimen was 23% of the total mass.

Three-Story Hybrid Simulation

Two dynamic excitations were used in this three-story RTHS. One was a banded white noise acceleration history with a frequency range of $0.1 \sim 10$ Hz and unity amplitude. The time series has a resolution of 1024 Hz and a duration of 60 s. The other excitation was the measured ground acceleration from the Northridge earthquake used in the numerical simulation. Because the object of this test was to validate the general formulation of RTHS method and the RTHS controller developed, it was desired to avoid inelastic deformation of the specimen during the test. Therefore, the dynamic excitations' amplitude was scaled on the basis of the simulation results to ensure repeatable and elastic responses of the specimen.

The actuator driving the shake table was controlled in displacement because of the limitation of the MTS controller, and the general formulation was derived based on acceleration control. The desired base acceleration was therefore doubly integrated to obtain the displacement command before the test, making it infeasible to implement a closed-loop substructure formulation of RTHS using specimen's responses feedback to compute the base acceleration input. A double integration method was developed to convert the acceleration signal to the displacement command in the frequency domain and then transformed back to the time series. For the low-frequency content of the acceleration input, the aforementioned process would generate large-amplitude displacement command that exceeded the shake table's actuator stroke. A high-pass cutoff frequency was set at 0.5 Hz prior to the double integration to maintain the displacement command within the limit. As a result, bias was introduced in the simulated and measured responses, which will be discussed subsequently in the test results.

Five implementation cases were physically tested as listed in Table 3, among them four cases were numerically simulated except for the PSD testing (Case 2N). This was caused by the setup limitation in connecting the actuator directly to the damping and stiffness components of the experimental substructure. Case 1 was a quasi-dynamic testing with the reduced-mass model loaded by the dynamic actuator only. Cases 2 through 5 were dynamic testing on the full-mass model. Case 2 tested the full-hybrid case with dynamic loads applied at the base and the top of the substructure equally. In Case 3, all the dynamic loads were applied through the dynamic actuator representing an effective force substructuring testing while in Case 4, all the dynamic loads were applied through the base motion alone as a shake table substructuring test. Finally, in Case 5 the RTDHS was implemented with the dynamic loads applied at the base and at the top as they were simulated. It is noted that Case 4 was unsuccessfully attempted by Reinhorn and Kunnath (1989).

Test Results and Discussion

The transfer functions of the relative responses of the second story to the first story $(x_{21}/\ddot{x}_{21})$ with respect to the white noise input were obtained using the MTS-STS frequency analyzer for five implementation cases, as shown in Figs. 10 and 11 for displacement and acceleration, respectively. They are compared with two simulation results: (1) the computational result obtained from the numerical model of the three-story structure (on the basis of dynamic properties listed in Table 2) with the toolbox provided by MATLAB/Simulink; and (2) the real-time simulation result obtained using the STS frequency analyzer from the same numerical model but downloaded to *xPC Target* (real-time system operator). Observations on these transfer functions are described as follows:

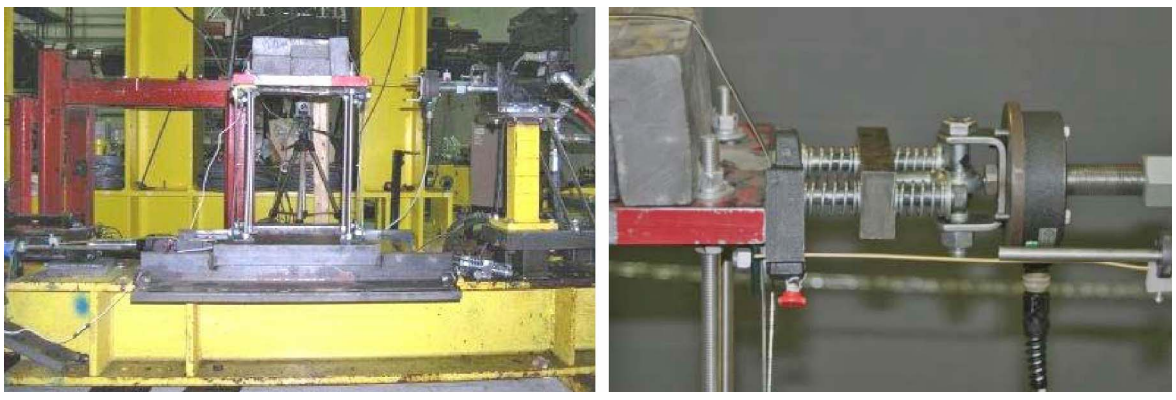

Fig. 9. Three-story hybrid simulation setup

J. Struct. Eng., 2011, 137(7): 748-760

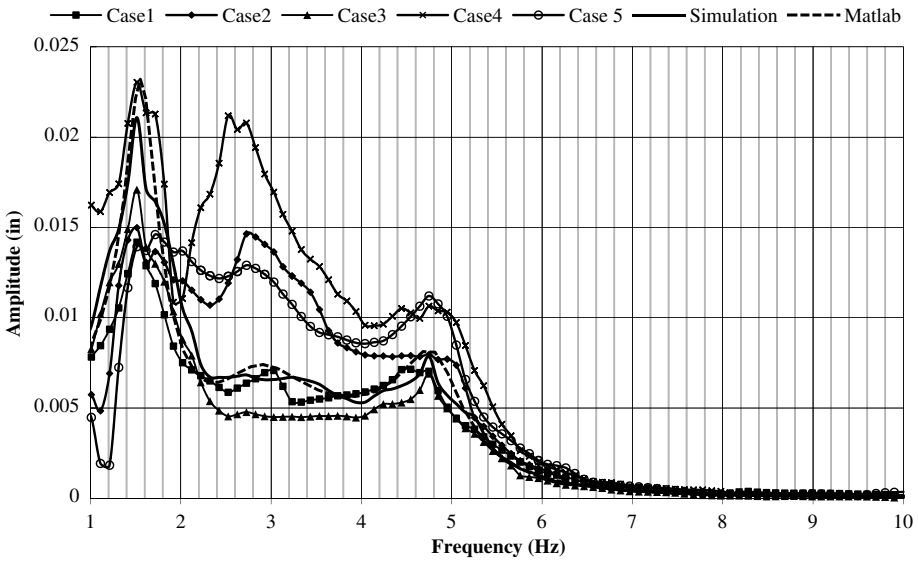

Fig. 10. Second-story relative displacement (x_{21}) frequency response

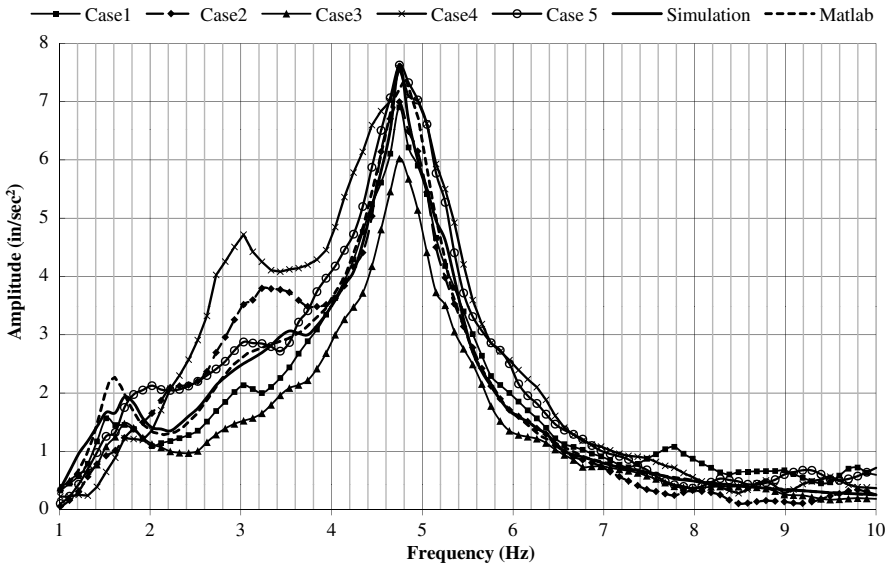

Fig. 11. Second-story relative acceleration ($\ddot{x}_{21}$) frequency response

The transfer functions obtained from MATLAB/Simulink and from simulation have minimal differences. Except for the minor difference around the natural frequencies, the real-time simulation reasonably reproduced the theoretical model behavior, proving that the way of generating transfer functions using STS frequency analyzer is reliable. The minor difference is attributed to minimal damping introduced to the system by the digital analysis tools, such as delays in data sensing and transfer.

The response transfer functions of displacement and acceleration showed clearly two peaks at 1.5 and 4.8 Hz, which are the first and the third natural frequencies of this three-story model. They matched very well to the numerical results in Fig. 10, which are 1.55 and 4.87 Hz respectively. The errors between the numerical and experimental results were less than 4%. The second natural frequencies measured from different loading implementation cases were moderately different ranging from approximately 2.6 to 3.0 Hz for two reasons. One reason is that the second vibration mode of this three-story model is not a dominate mode as can be seen from the analytical response (MATLAB/Simulink). A flat peak is observed around the second natural frequency 2.9 Hz with small amplitude. The other reason is that the second natural frequency of the three-story model is close to the natural frequency of the SDOF physical specimen (2.7 Hz). These two reasons made the specimen sensitive to the imperfect compensation controller and biased base motion input from the shake table at the second natural frequency. Nevertheless, we may conclude that the results obtained from the RTHS are able to capture the natural frequencies of the global three-story structural model, although only the second story was physically tested.

The amplitudes of displacement and acceleration frequency responses in all cases are not identical to the simulation results. Smaller discrepancies were observed at the first and the third natural frequencies compared with a much larger discrepancy at the second natural frequency. The major reason for this discrepancy is caused by displacement control of the shake table instead of desired acceleration control. Comparing the achieved displacement and acceleration motion of the shake table in the frequency domain (see Fig. 12), one may notice that the displacement contains

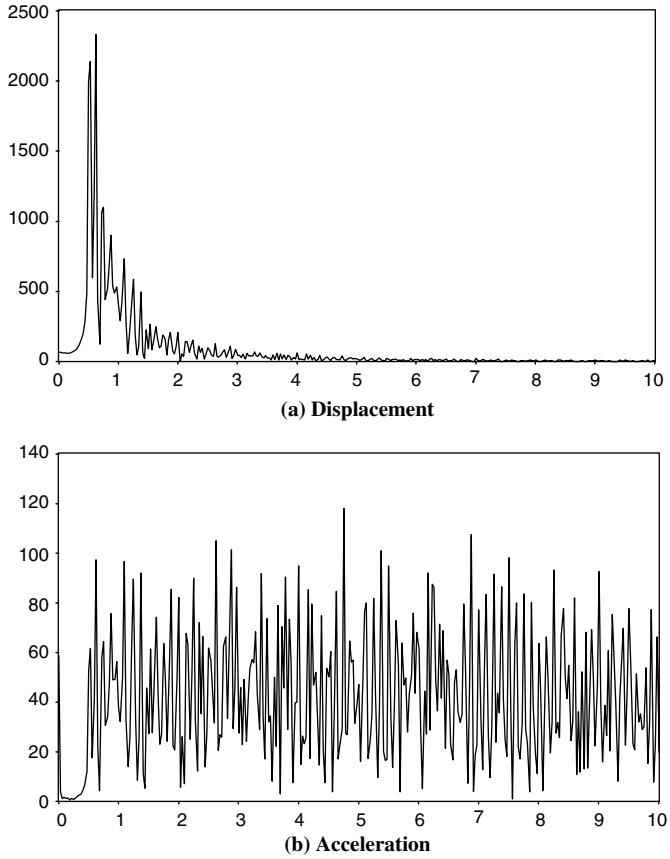

Fig. 12. Fast Fourier transformation of the shake table motion with white noise input

significant low-frequency content than the uniformly distributed acceleration frequency content from 0.5–10 Hz. The uniformly distributed acceleration input resulted in consistent acceleration responses of the experimental substructure in both amplitudes and natural frequencies. In addition, the actuator being serial connected to the specimen introduced additional damping to the whole test system, beside the structural damping. This additional damping will alter the responses, particularly decreasing the response amplitudes as substantiated by Case 3 and Case 1 when only the actuator is used to impose the dynamic loading. An improved compensation controller is the topic of current research to minimize the effect of the additional damping to the test system.

A portion of the measured displacement responses time history of the second-story drift relative to the first story subjected to Northridge earthquake excitation are shown in Fig. 13 for five cases and compared with the numerical simulation result (the thinner line in each plot). All measured displacement responses exhibit a good match to the simulated one, showing that different cases derived from the general formulation produced similar structural responses in RTHS. Therefore, the general formulation is feasible and effective. The dynamic actuator was capable of applying the desired force to the specimen using the developed force control strategy. The response under shake table input only (Case 4) approximately matched the simulation result caused by the aforementioned limitation of the shake table controller. The tests conducted with the dynamic actuator only (i.e., Case 1 and Case 3) show the best match to the numerical simulation with almost identical amplitude and approximately 7 ms delay in response. This delay is equivalent to the time delay of the actuator's response, demonstrating the efficiency of the Smith's predictor compensation method in eliminating the time-delay effects from the physical test results.

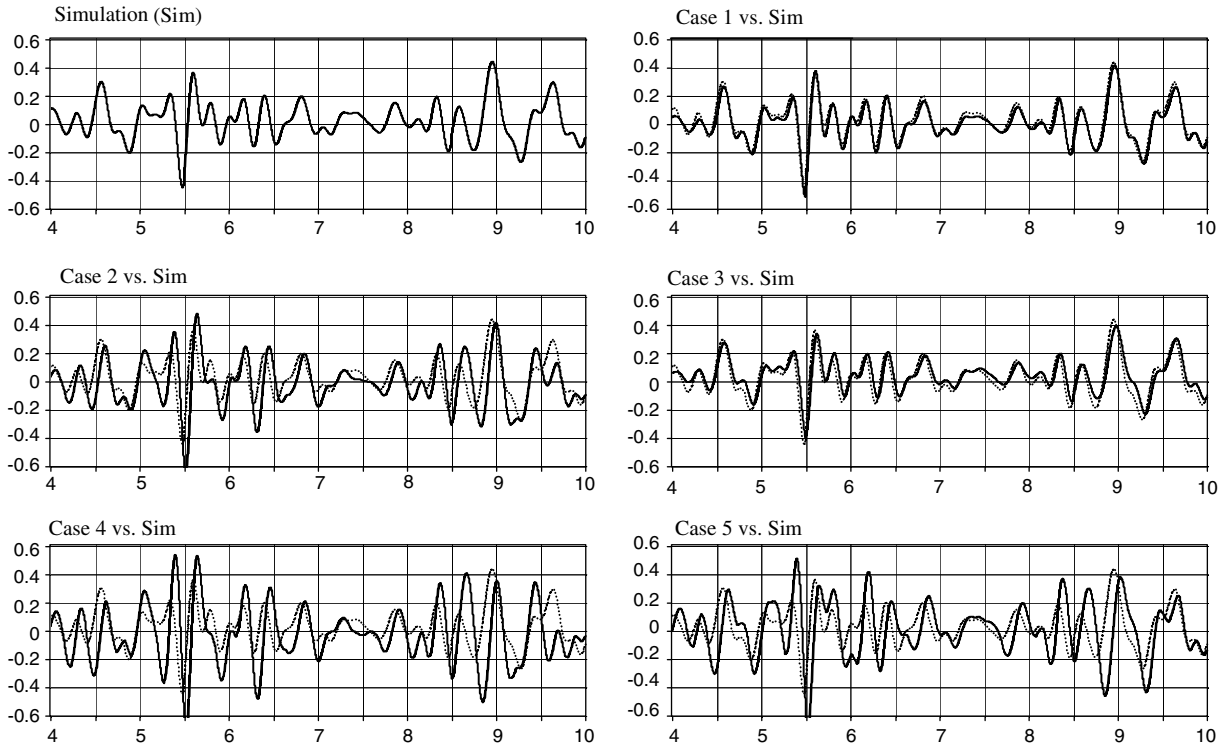

Fig. 13. Second-story relative displacement (x_{21}) time history

J. Struct. Eng., 2011, 137(7): 748-760

The physical test responses of the experimental substructure in both time and frequency domain proved the concept of the RTHS method, in that the measured responses obtained from a portion of the structure that is physically loaded by both shake tables and actuators with the loading command determined from the substructure formulation are comparable to the numerical simulation result when such portion is simulated within the whole structural model. In addition, the general formulation representing various hybrid simulation methods was also validated. The differences among the measured responses and the simulation results, especially when the shake table was used to provide part or all of the dynamic loading, were mainly caused by the limitation of the shake table controller.

Concluding Remarks

RTHS is a seismic testing method for large-scale structures. The method combines the numerical simulations of one or more computational substructures and the physical testing of a possible nonlinear experimental substructure. Both shake tables and actuators are employed to apply seismic loading to the physical specimen, enabling a dynamic testing of the substructures being executed at the real-time rate and generating real inertial effects while considering the whole system. The substructure and the general formulation of RTHS are derived showing its applicability to include versatile seismic testing methods. The modular architecture of the controller platform developed for the conventional real-time dynamic hybrid simulation was adopted with minor modification in implementing the general formulation. The numerical simulation and the physical experiment of a three-story RTHS conduced with five implementation cases defined by the general formulation demontsrated the versatility of the RTHS method while still generating reliable global structural responses.

Acknowledgments

This work was made possible by the National Science Foundation (NSF) grant CMS0086611 and CMS0086612. The authors acknowledge the financial support.

References

Ahmadizadeh, M., Mosqueda, G., and Reinhorn, A. M. (2008). "Compensation of actuator delay and dynamics for real-time hybrid structural simulation." *Earthquake Eng. Struct. Dyn.*, 37(1), 21–42.

Chen, C., and Ricles, J. M. (2009). "Improving the inverse compensation method for real-time hybrid simulation through a dual compensation scheme." *Earthquake Eng. Struct. Dyn.*, 38(10), 1237–1255.

Darby, A. P., Blakeborough, A., and Williams, M. S. (1999). "Real-time substructure tests using hydraulic actuator." *J. Eng. Mech.*, 125(10), 1133–1139.

Dimig, J., Shield, C., French, C., Bailey, F., and Clark, A. (1999). "Effective force testing: A method of seismic simulation for structural testing." *J. Struct. Eng.*, 125(9), 1028–1037.

Ji, X., Kajiwara, K., Nagae, T., Enokida, N., and Nakashima, M. (2009). "A substructure shaking table test for reproduction of earthquake responses of high-rise buildings." *Earthquake Eng. Struct. Dyn.*, 38, 1381–1399.

Kausel, E. (1998a). "New seismic testing method. I: Fundamental concepts." *J. Eng. Mech.*, 124(5), 565–570.

Kausel, E. (1998b). "New seismic testing method. II: Proof for MDOF systems." *J. Eng. Mech.*, 124(5), 571–575.

Kunnath, S. K., and Reinhorn, A. M. (1989). "Inelastic three-dimensional response analysis of RC buildings (IDARC 3-D) Part I—Modeling." *Technical Rep. NCEER-89-0009*, National Center for Earthquake Engineering Research, SUNY/Buffalo.

Lee, S.-K., Park, E. C., Min, K.-W., and Park, J.-H. (2007). "Real-time substructuring technique for the shaking table test of upper substructures." *Eng. Struct.*, 29(9), 2219–2232.

Mahin, S. A., and Shing, P. B. (1985). "Pseudodynamic method for seismic testing." *J. Struct. Eng.*, 111(7), 1482–1503.

Mercan, O., and Ricles, J. M. (2007). "Stability and accuracy analysis of outer loop dynamics in real-time pseudodynamic testing of SDOF systems." *Earthquake Eng. Struct. Dyn.*, 36(11), 1523–1543.

MTS Systems Corporation 2003793.xx. [Computer software]. (2003). MTS Systems Corporation.

Nakashima M., Kaminosono N., Ishida M., and Ando K. (1990). "Integration techniques for substructure pseudo dynamic test." *Proc., 4th U.S. National Conf. on Earthquake Engineering*, 2, CA, 515–524.

Nakashima, M., Kato, H., and Takaoka, E. (1992). "Development of real-time pseudo dynamic testing." *Earthquake Eng. Struct. Dyn.*, 21(1), 79–92.

Mathworks. Simulink and xPC target. (2003). [Computer software]. Mathworks.

Neild, S. A., Stoten, D. P., Drury, D., and Wagg, D. J. (2005). "Control issues relating to real-time substructuring experiments using a shaking table." *Earthquake Eng. Struct. Dyn.*, 34(9), 1171–1192.

Reinhorn, A. M., Bruneau, M., Chu, S. Y., Shao, X., and Pitman, M. C. (2003). "Large scale real time dynamic hybrid testing technique—Shake tables substructure testing." *Proc., ASCE Structures Congress*, Seattle, Paper 587.

Reinhorn, A. M., Sivaselvan, M. V., Liang, Z., Shao, X., Pitman, M., and Weinreber, S. (2005). "Large scale real time dynamic hybrid testing technique—Shake tables substructure testing." *Proc., 1st Int. Conf. on Advances in Experimental Structural Engineering*, AESE, Nagoya, Japan, 457.

Shao, X. (2007). "Unified control platform for real time dynamic hybrid simulation." Ph.D. dissertation, Dept. of Civil, Structural and Environmental Engineering, State Univ. of New York, Buffalo.

Shield, C. K., and French, C. W. (2001). "Development and implementation of the effective force testing method for seismic simulation of large-scale structures." *Philos. Trans. R. Soc. A*, 359(1786), 1911–1929.

Shing, P. B. (2008). "Real-time hybrid testing techniques." *Modern testing techniques for structural systems dynamics and control*, O. S. Bursi and D. J. Wagg, eds., CISM-Springer Wien, New York.

Shing, P. B., Nakashima, M., and Bursi, O. S. (1996). "Application of pseudodynamic test method to structural research." *Earthquake Spectra*, 12(1), 29–56.

Shing, P. B., Wei, Z., Jung, R. Y., and Stauffer, E. (2004). "Nees fast hybrid test system at the University of Colorado." *Proc., 13th World Conf. on Earthquake Engineering*, Vancouver, Canada, Paper No. 3497.

Sivaselvan, M. V., Reinhorn, A. M., Shao, X., and Weinreber, S. (2008). "Dynamic force control with hydraulic actuators using added compliance and displacement compensation." *Earthquake Eng. Struct. Dyn.*, 37, 1785–1800.

Stojadinovic, B., Mosqueda, G., and Mahin, S. A. (2006). "Event-driven control system for geographically distributed hybrid simulation." *J. Struct. Eng.*, 132(1), 68–77.

Wallace, M. I., Sieber, J., Neild, S. A., Wagg, D. J., and Krauskopf, B. (2005). "Stability analysis of real-time dynamic substructuring using delay differential equation models." *Earthquake Eng. Struct. Dyn.*, 34(15), 1817–1832.

Wu, B., Bao, H., Ou, J., and Tian, S. (2005). "Stability and accuracy analysis of the central difference method for real-time substructure testing." *Earthquake Eng. Struct. Dyn.*, 34(7), 705–718.